

# SPECIFIC OPERATION MODES AT THE METROLOGY LIGHT SOURCE

J. Feikes<sup>†</sup>, P. Goslawski, J. Li, M. Ries, M. Ruprecht, G. Wüstefeld, HZB, Berlin, Germany  
 A. Hoehl, Physikalisch-Technische Bundesanstalt (PTB), Berlin, Germany

## Abstract

The high flexibility of the Metrology Light Source (MLS) allows application of various nonstandard user modes adapted to the specific needs of their users. We report on some of them including a mode for division of the revolution frequency for the user signal and a mode with an adjustable photon pulse delay on the few ps scale.

## INTRODUCTION

The MLS [1] is a ramped 630 MeV synchrotron radiation source consisting of 4 DBA structures (Table 1) located in Berlin, Germany next to BESSYII. It is owned by the German national metrology institute PTB, and in contrast to most other synchrotron radiation sources it is used by the same institute. This allows to decide very flexible on the desired operation modes. Presently there are seven beam lines in operation. Figure 1 gives an overview of the corresponding fields of activity. The operation of the MLS is highly automated on a “one push button” base [3]. A desired operational mode is selectable from a list of options (by now six) and a change of mode can be realized within seconds (or minutes if new injection and ramping is desired). The beam current is conserved on changes between different modes. This flexibility in operation allows machine operation in adapted modes for special user requirements reported here. Because of its small revolution time it is not possible to operate the MLS with a sufficiently large bunch gap to avoid ion trapping. The vertical beam size is thus dominated by fast, ion driven instabilities, and varies strongly with the beam current.

Table 1: Machine and Operating Parameters of the MLS

Circumference	48 m
Revolution frequency	$f_{rev} = 6.25$ MHz, $T_{rev} = 160$ ns
Injection Energy	105 MeV
Operational Energy	50 MeV to 630 MeV
Beam Current	1 pA (1 e-) to 200 mA
Momentum Compaction Factor $\alpha$	$-5 \times 10^{-2} < \alpha < 5 \times 10^{-2}$
emittances at 630 MeV	25 nmrad (low emittance) 100 nmrad (standard user)
Typical lifetimes in different operation modes	Standard 6 h @150 mA 30 h @1 pA (1 e-) Low emit. 2 h @150 mA Low Alpha 10 h @150 mA

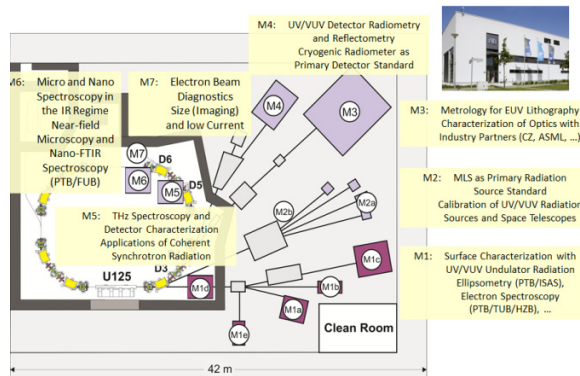


Figure 1: MLS beam lines and fields of application.

## SPECIFIC USER MODES

### Standard User Mode and Low Emittance Mode

The standard user mode is optimized for temporal and spatial stability and offered during 60% of the total annual user time.

In standard user mode a horizontal white noise excitation with varying amplitude (its value is set by a beam current dependent feed forward controller) equalizes the current dependency of the source size. In contrast the low emittance mode, mainly used for the operation of a scanning near field optical microscope s-SNOM, provides a constant brightness over time. In this mode therefore the vertical source size is adjusted to drop linearly with beam current (Fig. 2) to keep the brilliance constant.

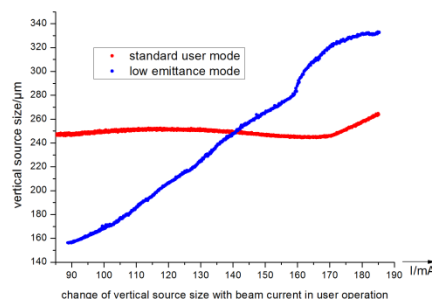


Figure 2: Typical behaviour of the vertical source size with beam current in standard and low emittance mode. There are slight differences from run to run depending on the homogeneity of the filling.

### Standard Low Alpha Mode

By design the MLS is equipped with octupoles, additional families of sextupoles, and individual powered quadrupoles, optimized for a low alpha operation [1, 2]. In low alpha mode the bunch length varies from 1 ps to 10 ps, mostly with beam currents well above the bursting

threshold to achieve high THz power, up to the max. current of 200 mA. An example for an application in this mode is shown in Fig. 3, where the time response of fast Schottky diodes with high sensitivity in the THz/FIR regime, was characterized.

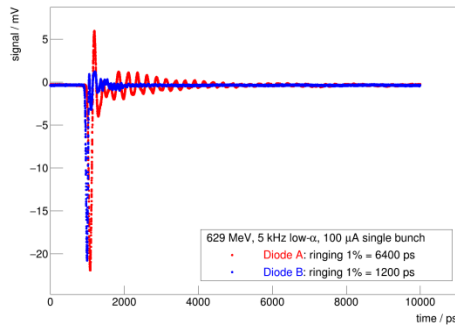


Figure 3: Time response of two fast THz/FIR (Schottky) diodes to the very short THz-radiation pulse in low alpha mode. The duration of the output pulses are minimized thus developing detectors for very short THz pulses as they typically arise at synchrotron light sources.

### Negative Low Alpha Mode

The bursting thresholds in a negative low alpha mode are lower than those of positive alpha mode [2]. There was some suspicion that the spectral distribution well above the bursting threshold could be broadened. As this would be advantageous for THz applications, strong efforts were spent to realize a high current negative low alpha application mode. For an energy-ramped machine like MLS it is very difficult to change the sign of the rf-gradient at the synchronous phase. Therefore a new injection state and a corresponding energy ramp had to be realized allowing offering presently up to 100 mA beam current to users in negative alpha mode. For this it was crucial, that not only the transverse chromaticities had to be set to negative values. Also the sign of longitudinal chromaticity had to be changed to a (small) negative value. Otherwise strong head-tail like instabilities prevents storage and ramp of higher beam currents than a few mA. It was found that the spectral distribution of the THz radiation at high currents does not depend on the sign of  $\alpha$  (Fig. 4), but, not surprisingly, on the beam current (Fig. 5).

### Delayed Alpha Buckets

The momentum compaction factor  $\alpha(p)$  can be expanded into power series of the momentum deviation  $\Delta p$ :

$$\alpha(\delta) \equiv \frac{\Delta L}{L} \frac{1}{\Delta p/p} = \alpha_0 + \alpha_1 \delta + \alpha_2 \delta^2 + \dots,$$

with  $L$  orbit length,  $p = p_0 + \Delta p$  momentum and  $\delta = \Delta p/p_0$  momentum deviation to the reference particle with momentum  $p_0$ . At the MLS,  $\alpha$  can be controlled up to second order.

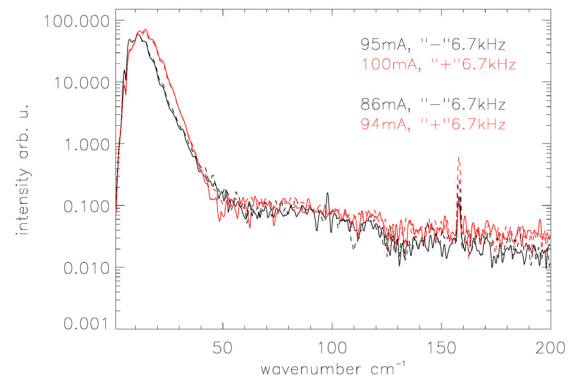


Figure 4: Comparison of THz spectra in negative (black) and in positive (red) low alpha mode on two different occasions well above the bursting threshold. No significant difference can be observed.

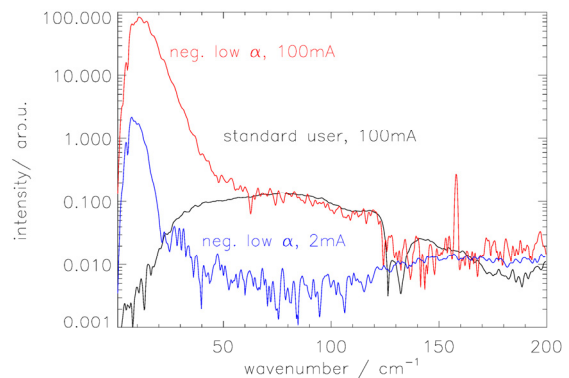


Figure 5: THz spectrum for a high (red) and low (blue) beam current value compared to the incoherent signal (black). Bursting broadens the spectrum.

By proper tuning, additional buckets develop in phase space, where electrons are stored at the same phase with respect to the cavity pass, but at different energies  $\delta_+$  and  $\delta_-$  (Fig 7).

The flexibility in the MLS lattice allows to adjust the path length variation with beam energy in one half of the ring ( $\alpha_I$ ) with a different sign than in the other half ( $\alpha_{II}$ ), so that the sum at  $\delta = 0$ , the value of  $\alpha_0$ , remains unchanged [2]. The so adjusted value of  $\alpha_0$  then determines the zero current bunch length. At the RF cavity both buckets have to arrive synchronously but as their different energies result in different path length in one half of the ring, the buckets pass the observation point at the ID-section at an (adjustable) time delay of up to 30 ps depending on the lateral position

$$\Delta T \approx \frac{\Delta L}{2\beta c} \alpha_I (\delta_+ - \delta_-)$$

$\Delta L$  - distance to cavity. This mode was realized, the bunch separation confirmed using a streak camera (Fig 8), and then used in an experimental setup. As the IR beam line, where the spectra were taken, is located closer to the RF cavity, the time separation there was limited to 6 ps.

*Sub-Revolution on Resonance*

There are activities at the MLS undulator beamline measuring photo emission with a time of flight spectrometer [5, 6]. Users were interested in enlarging the time interval between two incoming photon pulses to allow the photo-emitted electrons a longer travel distance thus increasing the resolution of their device.

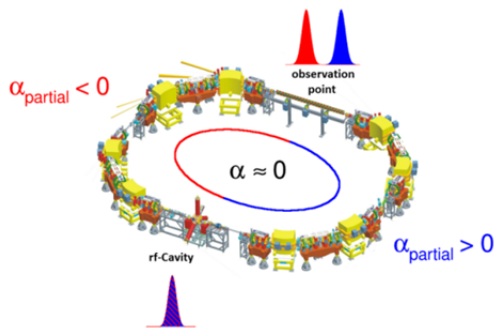


Figure 6: Principle of delayed bucket generation. At the observation point the alpha buckets corresponding to energies  $\delta_+$  and  $\delta_-$  pass with an adjustable longitudinal delay of up to  $\pm 30$  ps.

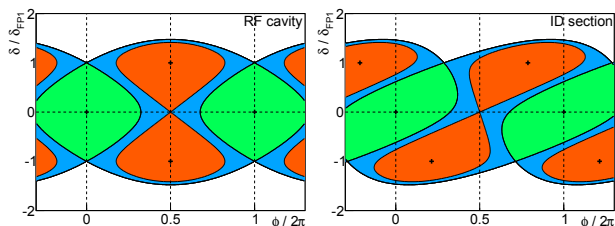


Figure 7: Example of longitudinal phase space for regular alpha optic (left) and delayed alpha bucket optic (right). The crosses in the area of closed trajectories (red areas) indicate stable fixed points, the upper corresponding to beam energies  $\delta_+$  and the lower one to  $\delta_-$ .

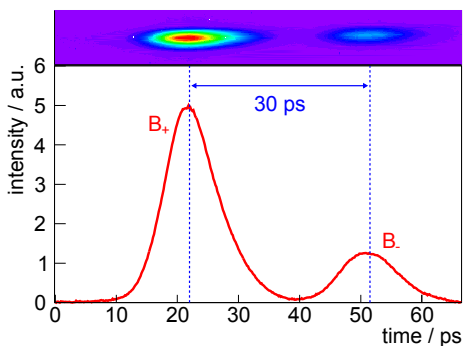


Figure 8: Streak camera measurement of delayed buckets with a time separation of 30 ps at the observation point.

A repetition time of 480 ns at the experiment could successfully be realized by operating the MLS on  $3^{rd}$  order resonance, and forcing the electrons into one of the three developing transverse buckets (Fig. 9), finally masking two of them relative to the experimental point. The method was described in detail in [4]. Using suitable apertures in the photon beam line and by steering properly the orbit

angle at the source point, a purity of the 2 MHz signal ( $f_{rev}/3$ ) at the 1% level (Fig. 10) could be achieved and 2MHz TOF spectrometry was successfully performed. The time stability of the experiment during two user runs, lasting about 10 h each, was as good as in standard user operation mode. The lifetime was even better than in standard user mode since a slightly larger emittance increased the dominant Touschek lifetime.

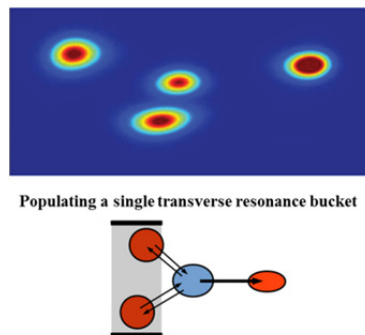


Figure 9: Source point image (visible light) of the transverse beam distribution at a tune near a  $3^{rd}$  order resonance. By non-linearly exciting the different transverse buckets all electrons of a single bunch can be driven into one single bucket. As the orbit closes only after 3 turns, the source point of this bucket also emits light only every  $3^{rd}$  turn.

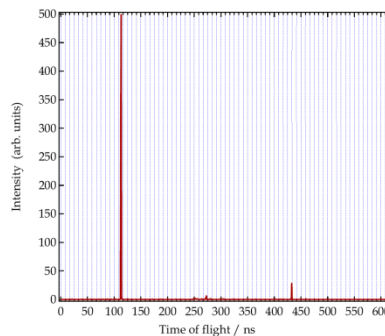


Figure 10: Arrival time of photo electrons emitted at a certain energy as seen by the TOF-spectrometer. The number of electrons emitted photons arriving in between three revolution periods in this example is as low as 7%, allowing full performance of the experiment. Courtesy of C. Lupulesco, W. Eberhard, HZB.

**ACKNOWLEDGEMENT**

We are very grateful to C. Lupulesco and Prof. Dr. W. Eberhard for sharing their results on TOF-spectroscopy.

**REFERENCES**

[1] J. Feikes et al. “The Metrology Light Source – The First Electron Storage Ring, Optimized for Generating Coherent THz Radiation”, Phys. Rev. ST Accel. Beams 14, 030705 (2011)  
 [2] M. Ries, “Nonlinear momentum compaction and coherent synchrotron radiation at the Metrology

Light Source – low-alpha commissioning and development”, PhD thesis, Humboldt-Universität zu Berlin, Germany

- [3] T. Birke et al, “Automated Operation of the MLS Electron Storage Ring”, in *Proc. PAC09*, Vancouver, Canada May 4-8, 2009, WE1RAC05 pp. 1798-1800.
- [4] M. Ries, “Transverse Resonance Island Buckets at the MLS and BESSY II”, in *Proc. IPAC2015*, Richmond, VA, May 2015, MOPWA021.
- [5] F. Roth et al., “Electronic properties of Mn-Phthalocyanine - C60 bulk heterojunctions: combining photoemission and electron energy-loss spectroscopy”, *J. Appl. Phys.* 118, 185310 (2015)
- [6] S. Weiß et al., “Exploring three-dimensional orbital imaging with energy dependent photoemission tomography”, *Nat. Commun.* 6, [open access], 8287 (2015)